Size limitations of quantum dot microdisc lasers

J. Molina Vázquez, R.W. Smink, B.P. de Hon, A.G. Tijhuis, G.D. Khoe and H.J.S. Dorren

Eindhoven University of Technology, P.O. Box 513, 5600 MB, Eindhoven, The Netherlands
(Email: j.molina.vazquez@ieee.org)

We calculate the whispering gallery modes in a microdisc laser with an InGaAsP/InP quantum dot gain medium. We find that the combination of large quantum dot gain bandwidth and strong field confinement provides support for several lasing modes. The effect of the microdisc dimensions on the lasing modes' properties is explored. Finally, we investigate the necessary microdisc and quantum dot properties to optimise the trade-off between the reduction in the microdisc's dimensions, which is required for high integration density, and the lasing modes' properties.

Introduction

The increasing speed of fibre-optic-based telecommunications has focused attention on high-speed optical processing of digital information. Complex optical processing requires a high-density, high-speed, low-power optical memory. Recently, a fast, low-power optical memory element based on coupled micro-ring lasers occupying an area of 720 μm^2 was demonstrated [1].

Semiconductor microdisc lasers are of great interest because of their small cavity volume, high cavity quality factors for whispering gallery modes, cleavage-free cavities, excellent wavelength selectivity and ultralow threshold [2]. These characteristics can be enhanced by using quantum dots (QDs) in the semiconductor's gain medium since they offer fast response to external pumping [3], low threshold, high characteristic temperature and large gain bandwidth [4].

During the last decade, whispering gallery modes in microdisc lasers have been theoretically and experimentally investigated [2,3,5–7]. However, the theoretical models in [5–7] are simplified to a two-dimensional problem neglecting the wavevector dispersion in the axial direction. In addition, these models have not been used to explore the size limitations of microdisc lasers, which is crucial in determining their integration potential for large scale memory applications. Finally, to the best of our knowledge, there has been no theoretical investigation of microdisc lasers in the full three-dimensional space with a QD active region.

Model

We consider a disc with a dielectric-air boundary supported by a post with an active region consisting of ten QD layers as that depicted in Fig. 1. Lower order modes suffer from large losses due to their low confinement within the disc. Hence, we are only interested in high order modes where the light propagates along the edge of the disc, and therefore the coupling of the field into the supporting post can be neglected. Due to the symmetry of the problem, we use a cylindrical coordinate system. This imposes Bessel-type solutions for the field in the radial direction. We solve Maxwell's equations in three dimensions,

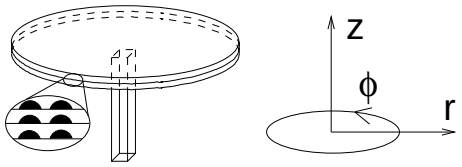

Fig. 1. Multiple layered quantum dot microdisk laser and coordinate system.

for transverse electric (TE) modes, using the method of Borgnis' potentials [8]. In the angular direction we assume clockwise and counter-clockwise propagating plane waves. In the axial direction the field consists of a cosine solution inside the disc and decaying exponential functions outside. Finally, in the radial direction the field is described by Bessel functions of complex order k_ϕ.

Note that the order of the Bessel is equal to the wavevector for the field propagating in the angular direction. Hence, in order to account for the losses due to the field radiating out of the disc, one must solve the field equations for complex k_ϕ. In the literature, one finds simplified solutions consisting of Bessel functions of integer order [5–7], which results in an over-estimation of the field confinement.

The computation of the Bessel functions is an essential element in our model. Since both the order and argument of the Bessel function can be complex, we perform the computation of the Bessel functions using their integral representations [9] with well chosen integration paths as described in [10].

To calculate the QD steady state gain and carrier-induced refractive index change, we compute the susceptibility of the gain medium taking into account the QD inhomogeneous broadening due to different alloy composition, the different QD confined levels, and their corresponding dipole matrix elements [11]. The electronic structure of the QDs is given by an anisotropic parabolic confinement potential as suggested by photoluminescence spectra [12]. The anisotropy in the confinement potential arises from the disc-shape of the dots giving stronger confinement in the growth direction. Finally, the polarization dephasing due to carrier-carrier interaction via Auger processes is calculated as in [13,14].

Results

Fig. 2 shows the calculated QD gain and carrier-induced refractive index dispersion for 10 layers with a QD density of 4×10^{10} cm^{-2} having 105 meV ($\sim$180 nm) energy level separation, which can be achieved using small size QDs. The gain and index can be scaled proportionally to the number of QD layers. The background index is 3.390, which corresponds to that of $In_{0.72}Ga_{0.28}As_{0.61}P_{0.39}$ [15]. A carrier density of 10^{12} cm^{-2} provides gain in both the ground and excited states. Also shown, are different lasing modes that can co-exist due to the broad gain bandwidth. Other modes are also obtained but their low field confinement within the disc and small spectral overlap with the QD gain forbids them from lasing. Due to the small carrier-induced refractive index from the QDs, the microdisc mode profiles are predominantly determined by the microdisc's material index and dimensions. Hence, one can modify the QD properties to provide the largest gain at the mode wavelength of interest. For example, one could engineer QDs with a gain spectrum that matches the 8^{th} and 10^{th} modes shown in Fig. 2, which are close to the

telecommunications wavelengths of 1.30 μm and 1.55 μm.

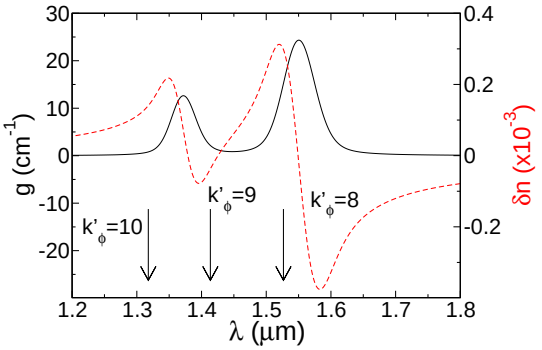

Fig. 2. Quantum dot gain (solid) and carrier-induced refractive index (dashed) spectra. Also shown are the lasing modes for the 1 μm radius and 200 nm height disc.

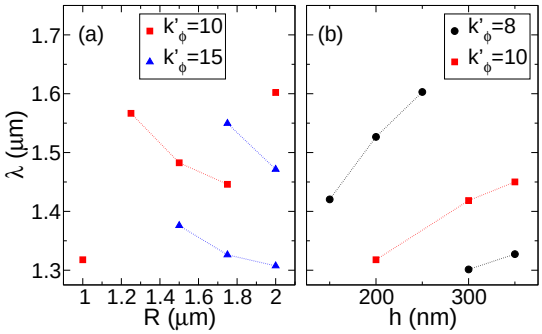

Fig. 3. Mode wavelength dependence on (a) disc radius, and (b) disc height, for the 8th (circles), 10th (squares) and 15th (triangles) modes. The lines give an aid to the reader.

The radius of the disc is varied from 0.50 μm to 2.00 μm for a fixed disc height of 200 nm, and the height is varied from 50 nm to 350 nm, for a fixed radius of 1 μm. Fig. 3 shows the mode wavelength dependence on the disc radius and height for modes within the wavelength range of 1.30 μm to 1.70 μm. It is clear how the mode wavelength decreases with increasing radius and increases with increasing height. We found that for disc radii below 1 μm or disc heights smaller than 200 nm there are no lasing modes. This is because only low order modes, whose field confinement inside the disc is low and correspondingly have large loss, can exist in the microdisc within the chosen wavelength range. Note that the modes in Fig. 3 will not always correspond to a lasing mode since this will depend on the QD gain at a particular wavelength. However, as mentioned earlier, one can tune the QD properties to provide better overlap between the gain spectrum and the mode of interest. From these results, one can calculate that the smallest memory element based on coupled QD microdisc lasers will have an area of $\sim$6.28 μm^2 and a thickness of 150 nm for the given material.

Finally, Fig. 4 shows the mode profiles for the 7th, 11th and 15th modes in the disc with 1.50 μm radius and 200 nm height. One can see the formation of whispering gallery modes for the higher order modes [Figs. 4(a) and 4(b)], with very low losses due to the strong field confinement.

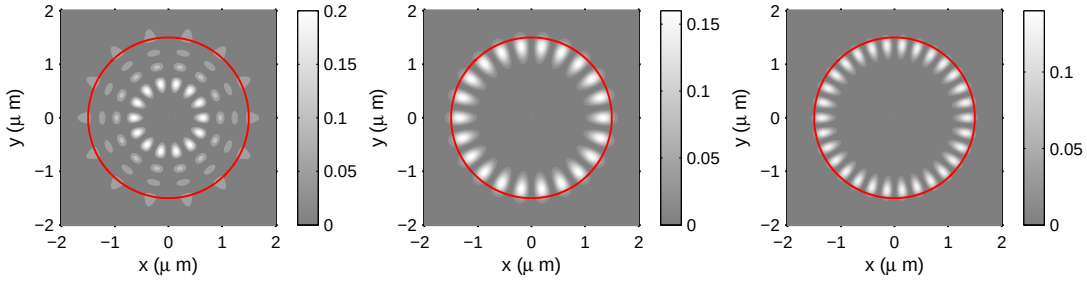

Fig. 4. Quantum dot microdisc laser (solid ring) modes with $k'_\phi = 7$ (left), $k'_\phi = 11$ (centre), and $k'_\phi = 15$ (right) for a disc with 1.50 μm radius and 200 nm height.

Conclusions

The lasing modes in quantum dot microdisc lasers have been numerically calculated and the dependence of the mode wavelength on the disc radius and height explored. We found that the smallest memory element based on coupled quantum dot microdisc lasers will require an area larger than $\sim 6.28 \mu m^2$ and a thickness greater than 150 nm for the material studied. This shows that quantum dots microdisc lasers are promising candidates for high density, large scale optical memories.

References

[1] M.T. Hill, *et al.*, *Nature*, vol. **432**, pp. 206–209, 2004.

[2] M. Fujita, *et al.*, *Electron. Lett.*, vol. **36**, pp. 790–791, 2000.

[3] K. J. Luo, *et al.*, *Appl. Phys. Lett.*, vol. **78**, pp. 3397–3399, 2001.

[4] D. Bimberg, *et al.*, *IEEE J. Select. Topics Quantum Electron.*, vol. **3**, pp. 196–205, 1997.

[5] N. C. Frateschi and A. F. J. Levi, *J. Appl. Phys.*, vol. **80**, pp. 644–652, 1996.

[6] M. Fujita, *et al.*, *IEEE J. Select. Topics Quantum Electron.*, vol. **5**, pp. 673–681, 1999.

[7] E. I. Smotrova and A. I. Nosich, *Opt. Quantum Electron.*, vol. **36**, pp. 213–221, 2004.

[8] K. Zhang and D. Li, *Electromagnetic theory for microwaves and optoelectronics*, Springer, Berlin, 1998.

[9] N. M. Temme, *Special Functions: an Introduction to the Classical Functions of Mathematical Physics*, Wiley-Interscience, Chichester, 1996.

[10] R. W. Smink, *et al.*, *Proc. Int. Conf. Electromag. in Advanced Applications & European Electromag. Struct. Conf.*, ISBN 88-8202-094-0, pp. 931–934, 2005.

[11] J. Molina Vázquez, *et al.*, *Optical and Quantum Electronics*, vol. **36**, pp. 539–549, 2004.

[12] G. Park, *et al.*, *Appl. Phys. Lett.*, vol. **73**, pp. 3351–3353, 1998.

[13] H. H. Nilsson, *et al.*, *Phys. Rev. B*, vol. **72**, pp. 205331, 2005.

[14] J. Molina Vázquez, *et al.*, *IEEE J. Quantum Electron.*, vol. **42**, pp. 986–993, 2006.

[15] F. Fiedler and A. Schlachetzki, *Solid State Electron.*, vol. **30**, pp. 73–83, 1987.